# FRACTURE TOUGHNESS OF FERRITIC SPHEROIDAL GRAPHITE CAST IRONS

A. LE DOUARON*, R. LAFONT*, D. POULAIN+, C. CLOITRE+

* RNUR - Direction des Laboratoires - Boulogne Billancourt
+ SBFM - Direction Technique - Lorient

## ABSTRACT

Two competing technics are employed to fabricate ferritic spheroïdal cast irons. It has been found that the ductile toughness measured at 20°C depends upon the manufacturing process, where as brittle toughness (- 40°C) is independent. Ductile crack opening displacement $\delta_i$ is a function of the average distance d between the nodules for as cast irons, while $\delta_i$ is a constant for ferritized cast irons. During ferritized heat treatment, cohesion interfacial stress decreases. It explains a decohesion, at the interface between graphite nodules and ferritic matrix during elastic deformation for the ferritized cast irons.

## KEYWORDS

Toughness, critical interfacial stress,local hydrostatic pressure, as cast and ferritized irons, nodule.

## INTRODUCTION

Two competing technics are employed to make ferritic spheroïdal cast irons. The ferritic structure is obtained either directly in as cast by using melts with high silicon content (3,3 %) or after an additional anneal at 900°C with low silicon content (2,4 %) (ordinary spheroïdal cast iron). The mechanical properties usually studied such as yield strength, tensile strength, impact energy, fatigue limit are very similar for these two materials (Table 2).

Because of the increased utilization for critically stressed components, particularly in the automotive industry, it has become necessary to develop technics for fail Safe design which are applicable to this material. The classical mechanical properties of spheroïdal graphite cast irons have been comprehensively covered by a number of workers. However there has been very little investigations into the determination of fracture parameters such as fracture toughness $K_{IC}$, and till lately the proposed failure mechanisms have been based on tensile and impact test data.

In the present paper fracture toughness results on ferritic S.G.* as cast and ferritized irons of varying silicon contents will be presented. The effect of nodule spacing on the fracture toughness is also considered. The implication of the ferritized heat treatment for the mechanisms of ductile fracture initiation will be discussed.

---

* SG : spheroïdal graphite

## 1 - EXPERIMENTAL

### 1.1. Material

Tables 1 and 3 give the chemical composition and the metallographic details of the SG irons. "A, B, C, D, E, F" cast irons are inoculated in mold after being post inoculated in ladle. F cast iron is heat treated (850°C-900°C) to dissolve carbides. G iron is inoculated in mold heat treated at 900°C down cooled to 750°C then air cooled. The mechanical properties of the irons used are shown in Table 2. Tensile tests were conducted using plane strain specimen.

Table 1

Chemical Composition

| | % C | % Si | % Mn | % Mg |
|---|---|---|---|---|
| A | 3,07 | 2,77 | 0,22 | 0,045 |
| B | 3,08 | 3,19 | 0,21 | 0,040 |
| C | 2,96 | 3,56 | 0,23 | 0,040 |
| D | 3,02 | 3,90 | 0,23 | 0,035 |
| E/F | 3,10 | 3,35 | - | - |
| G | 3,60 | 2,60 | 0,20 | - |

| | Yield strength MPa | Ultimate tensile strength MPa | Tensile élongation | Mesnager impact energy kJ/m2 | Matrice Hardness HV 500 | Fatigue limit MPa | |
|---|---|---|---|---|---|---|---|
| A | 420 | 600 | 0,125 | 235 | 165 | 290 to 310 | as cast |
| B | 440 | 620 | 0,105 | 168 | 192 | | |
| C | 480 | 660 | 0,080 | 94 | 200 | | |
| D | 540 | 710 | 0,115 | 165 | 222 | | |
| E | 450 | / | / | 150 | / | | |
| F | 380 | 600 | 0,105 | 204 | 188 | 260 to 280 | ferritized |
| G | 310 | 510 | 0,085 | 155 | 205 | | |

Table 2 - Mechanical properties (20°C)

| | % Perlite | Nodule characteristics: number/mm2 | mean diameter µm | mean inter nodule spacing µm |
|---|---|---|---|---|
| A | 10 | 101 | 14,8 | 92 |
| B | 0,5 | 135 | 14,2 | 79 |
| C | 0,5 | 164 | 14,6 | 72 |
| D | 0,5 | 183 | 12,4 | 68 |
| E/F | 0 | 139 | 16,4 | 78 |
| G | 0 | 18,3 | 32 | 217 |

Table 3 - Metallographic details



### 1.2. Specimen design and preparation

For all this study we used standard single edge notched specimens FT 8. The thickness effects were studied in the range between 5 to 14 mm. Fatigue precracking was carried out on an electrohydraulic machine at low stress in accordance with the recommanded procedure for fracture toughness testing, that is to say $\Delta K \leq 19$ MPa$\sqrt{m}$ and $da/dn < 2\ 10^{-8}$ m/cycle. Final fracture was carried out on a conventionnal tensile machine at 0,5 mm/mn. Ductile crack initiation was detected by US signal variation.

### 1.3. Measurement of the apparent critical stress intensity factors $K_{IQ}$

We determine two apparent critical stress intensity factors $K_{IQ}$ at crack initiation and $K_{IM}$ at the maximum load $F_M$. All these measurements were not valid. We have always $F_M \geq 1{,}1\ F_Q$. ASTM conditions for initial crack length and thickness were satisfied only for D irons at - 40°C. Like NANSTAD, WORZALA and LOPER (5,6) we observe a little increase of $K_{IM}$ and $K_{IQ}$ with thickness (Figure 1). In the following of this study the thickness of the bend specimens is 9 mm. $K_{IQ}$ increases whith silicon percentage, at room temperature it was maximum for 3,3 % silicon (Figure 2).

### 1.4. Critical J integral values measurement

To obtain "valid" results in SG irons like other relatively tough material, we made an alternative measurement using small test specimens : critical J integral value $J_{IC}$. In plane strain for elastoplastic body K and J are related to :

$$JE = K_I^2 (1-\nu^2)$$

We determine J and $J_{IC}$ using compliance technique in accord to BEGLEY and LANDES propositions, relative crack length satisfied the conditions :

$$0{,}58 < a/W < 0{,}67$$

Table 4 gives the results. The fracture toughness of ferritized irons is constant between -40°C and + 20°C, typically 21 to 26 MPa$\sqrt{m}$. ROUSSEAU and FRANCOIS (1) have obtained the same results with similar ferritized irons (23 MPa$\sqrt{m}$).

The fracture toughness of as cast irons seems independent of silicon percentage (64 to 75 MPa$\sqrt{m}$ at room temperature) and decreases with temperature (26 to 18 MPa$\sqrt{m}$ at - 40°C).

| | | as cast irons A | B | C | D | ferritized irons F | G |
|---|---|---|---|---|---|---|---|
| + 20°C | $J_{IC}$ KJ/m2 | 32 | 28 | 32 | 26 | 3,9 | 2,8 |
| | $K_{IC}$ MPa$\sqrt{m}$ | 74,3 | 66,9 | 74,3 | 64,5 | 25,9 | 22 |
| - 40°C | $J_{IC}$ KJ/m2 | 4,1 | 3,3 | 2,9 | 2,1 | 3,6 | 2,9 |
| | $K_{IC}$ MPa$\sqrt{m}$ | 25,6 | 22,9 | 21,5 | 18,3 | 24,9 | 21,5 |

Table 4 - Critical $J_I$ integral values and $K_{IC}$ calculated values

## 2 - DUCTILE FRACTURE MECHANISM

### 2.1. Macroscopical aspects

We have never observed shear zone on fracture surface of toughness specimens. It would be possible to observe such shear zones by working under high hydrostatic pressure. It is the case for plane strain tension specimen (Figure 5) where local hydrostatic pressure is higher than in toughness specimen near the crack tip (1)(9).

All our experiments were under small scale yielding conditions. Ligament dimension was higher and mean distance between nodules lower than plastic zone radius (Tables 5 and 3).

| | | | | |
|---|---|---|---|---|
| Plane stress | calculated | 520 | 3850 | 900 |
| | measured | 600 | 3100 | 1100 |
| Plane strain | calculated | 173 | 1280 | 300 |
| | | after fatigue precracking | in as cast | in ferritized |
| | | | at crack initiation | |

Table 5 : Radius of the plastic zone mean values (in $\mu$m) - Measurements were made using brittle lacquer.

### 2.2. Microscopical aspects

Microscopical initiation depends upon the manufacturing process (Figure 3). Ferritized irons critical crack opening displacement $\delta_i$* was unaffected by the nodule spacing $\delta_i = 8{,}5\ \mu m$

For as cast iron $\delta_i$ was a linear function of the average between the nodule :

$$\delta_i = 8{,}5 + 0{,}4\ d \text{ in } \mu m$$

Crack initiation occurs during elastic deformation for ferritized irons. As cast irons must be plastically deformed in order that nucleation begins. If crack initiation begins at nodule matrice interface in toughness specimens, in plane strain tension specimen initiation depends upon the manufacturing process. For ferritized irons we observed decohesions in all the section of the specimen, whilst decohesions occur in the ferritic matrix near the nodule (Figure 4) in a littre zone of 80 $\mu$m near the fracture surface and form an enveloppe around the nodule in as cast irons. This enveloppe may be broken during final fracture (Figure 7).

### 2.3. Discussion

Local stress should reach a critical value $\sigma_i$ at the matric nodule interface in order to break the interface and nucleate micro crack. In an other study (10) we have shown than in the case of spheroïdal soft inclusions, such graphite nodule, in plasticaly deformed matrix, local stress was highest in the vicinity of inclusion. Micro cracks could be nucleated in this high stress zone if $\sigma_i$ was higher than the yield strength of the matrix. It is the case for as cast iron during tensile test. Micro crack nucleate during elastic deformation of ferritized iron during tensile test, local stress is highest at the interface nodule matrix. So we have :

$$\sigma_i > \sigma_E \quad \text{for as cast iron}$$

$$\sigma_i > \sigma_E \quad \text{for ferritized iron}$$

$$\text{and} \quad \sigma_E > \sigma_E \quad \text{(Table 2)}$$

as cast ferritized

We write

$$\sigma_i > \sigma_i$$

as cast ferritized

Lowest critical interfacial stress $\sigma_i$ for ferritized can be explained by microscopical observations (Figure 8). During ferritized heat treatement structure and nodule-matrix interface was modified. Graphite recristallized and interface became notched and hole seemed to be form near the surface nodule (8).

* $\delta_i$ was related to $J_{IC}$ in small scale yielding conditions by : $J_{IC} = 2\sigma_E \delta_i$



The critical stress $\sigma_i$ depends upon local hydrostatic pressure and is not a function of the radius of the nodule (7). In a bend toughness specimen local hydrostatic pressure near the crack (in the crack initiation area) is lower than in a plane strain tensile specimen (1,9). So critical stress $\sigma_i$ is lower in a toughness test than in a tensile test. It is more easily to nucleate crack at the interface nodule matrix in toughness specimen than in tensile specimen. The difference between these two tests can explain the two mechanisms of crack nucleation observed for as cast irons : at the interface nodule matrix during the tensile test, at the vicinity of the nodule during the toughness test.

## CONCLUSION

Classical mechanical test cannot differentiate two competiting technics to make spheroïdal cast irons. Fracture mechanics analysis shows that better to use as cast irons than ferritized irons, crack initiation resistance is highest. This difference was explained by nodule matrix interface deterioration during ferritized heat treatment.

## REFERENCES


1 - D. ROUSSEAU - WAGNER
Influence de la taille et de la répartition des nodules de graphite sur la rupture des fontes à graphite sphéroïdal ferritiques.
Thèse Université de Compiègne 1976.

2 - BOLLANI
Proprieta meccaniche delle ghise speroidali - Note FIAT, Mars 1975

3 - G. JOLLEY and S.R. HOLDSWORTH
Ductile fracture initiation and propagation in ferritic S.G. Cast iron
Fracture 1977, Volume 2, ICF 4, Waterloo Canada June 1977, pp 403-413

4 - S. NISHI and T. KOBAYASHI
Fracture machanical studies in instrumented charpy impact test of cast irons
I.C.S.M.A.4 Nancy 1976, conference proceedings, volume 2, pp 524-528

5 - R.K. NANSTAD and F.J. WORZALA and C.R. LOPER
Static and dynamic toughness of ductile cast iron
A.F.S. transactions 1975, pp 245-256

6 - R.K. NANSTAD and F.J. WORZALA and C.R. LOPER
The fracture characteristics of nodular cast iron
The metallurgy of cast iron, pp 789-807

7 - A.S. ARGON and J. IM and R. SAFOGLU
Cavity formation from inclusions in ductile fracture
Met. Trans. 1975, volume 8A, pp 825-837

8 - L. LEVY
Etude des interfaces matrice graphite dans les fontes à graphite sphéroïdal

9 - R.H. SAILORS
Relationship between tensile properties and microscopically ductile plane-strain fracture toughness.
Properties related to fracture toughness
ASTM STP 605, 1976, pp 34-61

10 - A. LE DOUARON
Unpublished Renault technical papers.

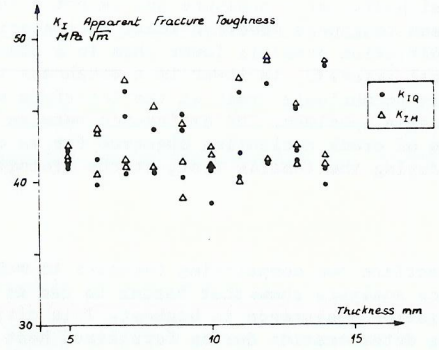


Fig. 1

Apparent fracture toughness (iron E)

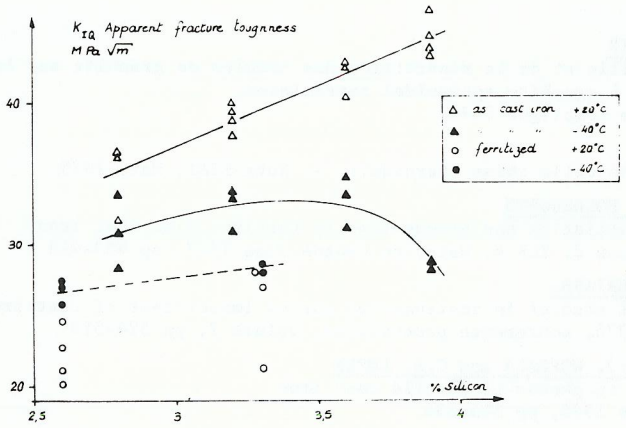


Fig. 2

Apparent fracture toughness

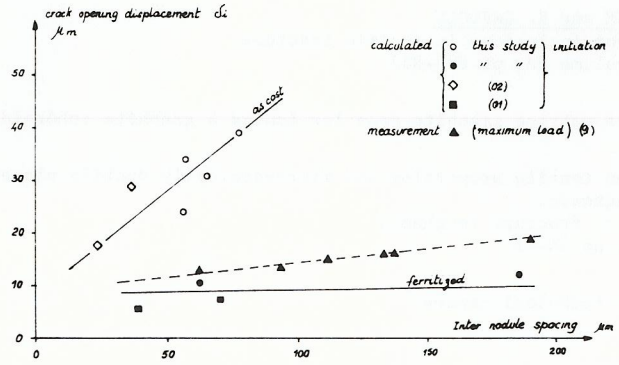


Fig. 3

Crack opening displacement



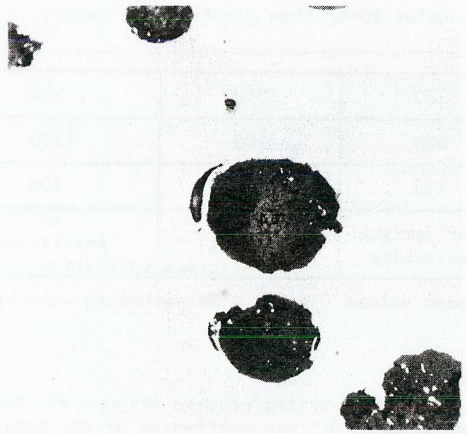


Fig. 4 : Crack initiation in as cast iron


Fig. 5 : Rupture and crack initiation in ferritized iron

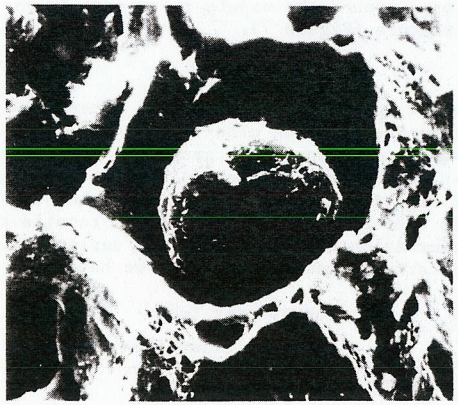


Fig. 6 : Ductile fracture in ferritized iron

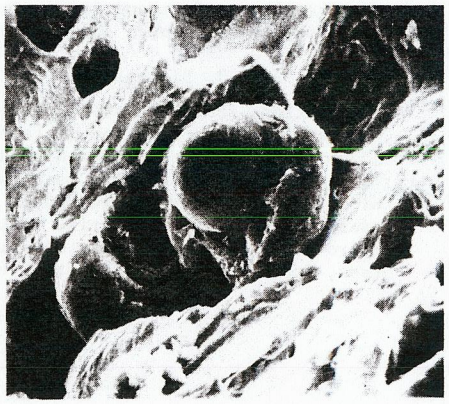


Fig. 7 : Ductile fracture in as cast iron

FERRITIZED IRON 1 µm

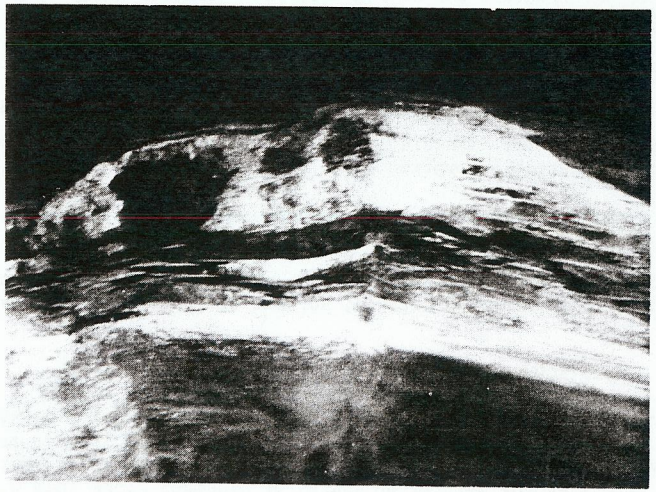

AS CAST IRON 1 µm

Fig. 8 : Interface between nodule and matrix